Research Article   **Open Access**

Ainaz Mihanfar, Niloufar Targhazeh, Shirin Sadighparvar, Saber Ghazizadeh Darband, Maryam Majidinia*, Bahman Yousefi*

Doxorubicin loaded magnetism nanoparticles based on cyclodextrin dendritic-graphene oxide inhibited MCF-7 cell proliferation

Abstract: Doxorubicin (DOX) is an effective chemotherapeutic agent used for the treatment of various types of cancer. However, its poor solubility, undesirable side effects, and short half-life have remained a challenge. We used a formulation based on graphene oxide as an anticancer drug delivery system for DOX in MCF-7 breast cancer cells, to address these issues. *In vitro* release studies confirmed that the synthesized formulation has an improved release profile in acidic conditions (similar to the tumor microenvironment). Further *in vitro* studies, including MTT, uptake, and apoptosis assays were performed. The toxic effects of the nanocarrier on the kidney, heart and liver of healthy rats were also evaluated. We observed that the DOX-loaded carrier improved the cytotoxic effect of DOX on the breast cell line compared to free DOX. In summary, our results introduce the DOX-loaded carrier as a potential platform for *in vitro* targeting of cancer cells and suggest further studies are necessary to investigate its *in vivo* anti-cancer potential.

Keywords: Breast cancer; doxorubicin (DOX); graphene oxide; apoptosis.

*Corresponding authors: Maryam Majidinia, Solid Tumor Research Center, Urmia University of Medical Sciences, Urmia, Iran, E-mail: majidinia.m@umsu.ac.ir; **Bahman Yousefi,** Molecular Medicine Research Center, Tabriz University of Medical Sciences, Tabriz, Iran; Department of Biochemistry and Clinical Laboratories, Faculty of Medicine, Tabriz, University of Medical Sciences, Tabriz, Iran, E-mail: yousefib@tbzmed.ac.ir
Ainaz Mihanfar, Department of Biochemistry, Faculty of Medicine, Urmia University of Medical Sciences, Urmia, Iran
Niloufar Targhazeh, Student Research Committee, Tabriz University of Medical Sciences, Tabriz, Iran
Shirin Sadighparvar, Saber Ghazizadeh Darband, Neurophysiology Research Center, Urmia University of Medical Sciences, Urmia, Iran

Introduction

Breast cancer is one of the most common malignancies and a major cause of mortality worldwide [1]. Surgical resection is common and often followed by adjuvant therapies, including chemotherapy and radiation, to eliminate any remaining cancer cells or those that may have spread to other parts of body after surgery. Conventional chemotherapeutic agents suffer from poor solubility, high systemic cytotoxicity, and lack of tumor selectivity in which may result in cancer treatment failure [2].

Doxorubicin (DOX) is one of the most effective drugs used for the treatment of breast cancer. Intrinsic and acquired resistance, undesirable side effects and short half-life require more rigorous approaches to combat these hurdles [3-7]. The fabrication of smart systems with various sensitivity to the changes of light, temperature, enzymes, pH and magnetic fields for protection of healthy tissue/organs from toxic drugs and to prevent denaturation of the agent to reach a specific site [8]. One strategy to improve tumor drug delivery is the entrapment of agents in a nanocarrier to increase effectiveness and control of delivery, termed a drug delivery system [8]. To date, several types of nanocarrier have been developed for drug delivery, including microspheres, liposomes, micelles, hydrogels, gold nanoparticles, magnetic nanoparticles, and polymeric dendrimers [9]. Numerous methods have been developed for the attachment of chemotherapeutic agents to the nanocarrier such as adsorption, encapsulation and covalent binding [10]. Recently, the use of multi-branched polymers and dendrimers has drastically increased due to their ability to improve drug efficiencies, higher drug loading capacity and ability to penetrate tumor tissue [11]. Iron oxide magnetic nanoparticles with desirable properties such as good biocompatibility, strong super para-magnetism and low toxicity, in combination with an external magnetic

field, have the potential to deliver particles to a specific area and release them locally [12]. Notably, hydrophobic coating limits the stability of magnetic nanoparticles and agglomeration of these iron oxide magnetic nanoparticles prevent immobilization of proteins and enzymes, therefore a suitable matrix such as carbon, chitosan or graphene is needed to overcome these obstacles [12]. Graphene oxide (GO), a derivative of graphene, with hydrophilic oxygen-containing groups allows for ease of functionalization and creates a favorable and versatile material for drug delivery systems and biosensor targets [13]. Due to the GO hydrophilic group vulnerability, various efforts have been considered for further functionalization and applicability of magnetic GO [14]. Recently, cyclic oligosaccharide, composed of seven D-glucopyranose units, β-cyclodextrin (β-CD), through a hydrophobic internal cavity and hydrophilic external cavity which could accommodate diverse organic and inorganic molecules opened up new avenues for surface modification and more effective drug delivery fabrication [10, 15]. Here, we aimed to increase the efficacy of DOX through the fabrication of a targeted delivery carrier of β-CD functionalized dendrimeric graphene oxide-magnetic nanoparticles. After these modifications, drug-loading, release properties, cellular uptake of the particles, and cell cytotoxicity in MCF-7 breast cancer cells were investigated.

Material and methods

Nanoparticle preparation

NPs were prepared as per the method developed previously [16]. Briefly, allyl imidazole grafted β-Cyclodextrin (Aly-Imz/CD) was prepared. Then the prepared Aly-Imz/CD was added to a mixture of alkyl halide N,N dimethylaminoethyl methacrylate (QDMAEMA) and 3-(trimethoxysilyl) propyl methacrylate (TMSMA) to synthesize the cationic nano-platform as a magnetic nanocarrier (Cat-MN) and then characterized.

Drug loading

To load DOX into the magnetic nanocarrier, 0.5 mg of 5-DOX and 50 mg of nanocarrier were added to a 5 mL PBS (pH 7.4) and stirred at room temperature in a sealed vial and protected from light for 24 h. Following the separation of the supernatant from the obtaining suspension after loading steps by an external magnetic

field, the amounts of unbounded DOX were determined using specific absorption wavelengths at 290 nm with a UV-VIS spectrophotometer. Then, the calibration curve for different contents of free DOX based on unloaded drug concentration was drawn in order to evaluate the concentration of DOX loaded into nanocarrier. Loading efficiency (LE) and encapsulation efficiency (EE) was calculated via equations 1 and 2, respectively:

$$\textbf{Eq. 1} \; LE \, (\%) = \frac{\text{mass of drug in nanocarrier}}{\text{mass of nanocarrier}} \times 100$$

$$\textbf{Eq. 2} \; EE \, (\%) = \frac{\text{mass of drug in nanocarrier}}{\text{mass of feed drug}} \times 100$$

DOX loading of nanoparticles,, as mentioned above, was performed continuously. The resultant precipitate (DOX/NPs) was washed with PBS and vacuum-dried.

Nanocarrier drug release

To evaluate DOX release from synthesized NPs, 4 mg of 5- DOX/NPs were dispersed in PBS buffer with two different pHs: pH5.0, to represent the acidic tumor microenvironment, and pH 7.4, to represent normal physiological conditions. An external magnetic field was applied to separate the supernatant. The absorbance of the supernatants was detected using a UV-VIS spectrophotometer at 290 nm. Finally, the drug release amount at any given time was calculated via equation 3.

$$\textbf{Eq. 3} \; \text{Drug release} \, (\%) = \frac{\text{mass of DOX in NPs}}{\text{mass of NPs}} \times 100$$

Cellular Uptake by Fluorescent Microscopy and Flow Cytometry

Cellular uptake of DOX/NPs was assessed by fluorescent microscopy and flow cytometry by labeling with Rhodamine-B, which gives a fluorescent feature to our platform and is a suitable approach for tracking the cellular uptake process. In evaluation by fluorescent microscopy, we seeded 20×10^3 MCF-7 breast cancer cells on a slide champers well. Then cultured cells were treated with DOX/NPs labeled with Rhodamine- B. After 2 and 4 h, cells were washed with PBS buffer and observed by fluorescent microscopy (Olympus microscope Bh2-RFCA, Japan). For flow-cytometry assessment of cellular uptake, we seeded 500×10^3 cells in a six-well plate and treated

with DOX/NPs labeled with Rhodamine-B for 2 and 4 h. After washing, cells were evaluated by a FACS caliber flow-cytometer to measure the fluorescent intensity.

In vitro cytotoxicity assay

Cell culture

Human breast cancer MCF-7 cells were obtained from the Pasteur Institute Cell Culture Collection (Tehran, Iran). Cells were cultured in RPMI-1640 supplemented with 10% FBS and 100 units/ml penicillin/streptomycin and maintained in a humidified incubator at 37°C in 5 % CO_2. The cells were passaged every 2–3 days to maintain exponential growth.

MTT assay

NP *in vitro* cytotoxicity was determined by MTT assay. In brief, MCF-7 cells were seeded at 96-well plates, and after 24 h treated with various concentrations of Blank NP, free DOX and DOX/NPs for 48 h. Experiments for each group were performed in triplicate and with a blank control. Then, the medium was removed and 200 µl RPMI-1640 medium supplemented with 10% FBS and 10% MTT (5 mg/ml) was added. After a 4 h incubation, the reduced intracellular formazan product was dissolved by replacing 100 µl of RPMI-1640 medium with the same volume of dimethylsuloxide (DMSO). Absorbance values were measured at 570 nm using a microplate reader (Biotek, ELx 800, USA). Plots of cytotoxicity index (%CI = (1-((OD treated)/(OD control)) × 100) vs. different concentrations of the inhibitor of signaling pathways were drawn. IC50 was determined from each plot by calculating the slope and intercept.

MitoTracker Green assay

A MitoTracker Green FM assay (Invitrogen, Germany) was used to determine mitochondrial mass as a marker of apoptosis following treatment with NPs, DOX, and DOX loaded NPs in MCF-7 cell lines. All processes were performed in accordance to the manufacturer's instructions. Briefly, after fixation with formaldehyde 10%, cells were incubated with a 100 nM MitoTracker Green FM for 45 min and then counterstained with 4', 6'-diamidino-2- phenylindole (DAPI). The coverslips were photographed utilizing the Olympus Fluorescence System

Microscope BX3-URA (Olympus Corporation, Japan), and 20 photos were taken randomly to ensure that the obtained data were representative. The percentages of MitoTracker-positive cells per total number of cells were counted and analyzed.

In vivo toxicity assay

Four-week-old normal Wistar rats were randomly divided into three groups based on body weight. Each group contained six rats and treated with free DOX, free NP, DOX/NP. Rats treated with physiological serum were considered the control group. Both DOX and DOX/NP administration dosages were 10 mg/kg of body weight via tail vein injection. The body weight and physical changes of the rats were monitored daily. After four days of treatment, blood was collected, and serum was isolated to determine biochemical parameters including, urea (Ur), creatinine (Cr), creatine kinase (CK), lactate dehydrogenase (LDH), alanine aminotransferase (ALT), and aspartate aminotransferase (AST). The experiments were conducted in accordance with ARRIVE guidelines (Animal Research: Reporting of In Vivo Experiments).

Statistical analysis

In this study, all values were demonstrated as mean ± SD. The Kolmogorov-Smirnov and Levene tests were applied for evaluating the normality of the data. One-way ANOVA POST HOC (Tukey and Dunnett) tests were applied to compare the mean between experimental groups. A P value of less than 0.05 was reported as statistically significant.

Results

In vitro DOX loading and release

The loading and release of DOX was evaluated at 37°C in PBS with varying pH (5.2 and 7.4). Encapsulation efficiency was 98.13% for DOX. The drug and nanocarrier formulation ratio was 1:10 drug loading efficiency in DOX was described 9.8%. Also, the release of DOX at pH 5.2 was 85% within 144 h while at pH 7.4, the release of DOX was 67%. The DOX release profile indicated quick release from the magnetic nanocarrier during the first 24 h (75% of the overall loaded DOX). These results clearly showed that

the pH value of the medium has a major effect on the DOX release rate from the magnetic nanocarrier and propose that DOX loaded nanocarrier sustained drug-nanocarrier electrostatic reactions under physiological conditions. Indeed, DOX loaded nanocarrier by electrostatic interactions, and the degree of protonation of the carboxyl groups in the magnetic nanocarrier was controlled by environmental pH, after most of the carboxyl groups in magnetic nanocarrier were protonated in low pH medium, the electrostatic interaction between magnetic nanocarrier with DOX was weakened, and therefore released from the nanoparticle. The pattern of release of DOX from magnetic nanocarrier was shown in figure 1.
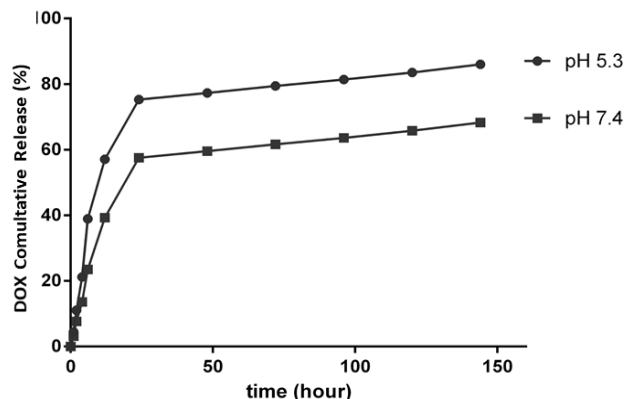

Figure 1: The cumulative release of DOX at various pH values (5.3 and 7.4) at 37°C.

Qualitative and quantitative analysis of cellular uptake

The nanocarrier's cellular uptake and internalization were estimated in a time-dependent manner using MCF-7 cells and fluorescence microscopy around the emission of red fluorescence of Rhodamine. As shown in figure 2, the Rhodamine-loaded nanocarrier, after 2 and 4 h, could be up taken efficiently and internalized by MCF-7 cells when compared with a free Rhodamine positive control. The uptake process was complete within the first 2 h, since fluorescence images revealed high fluorescence intensity within the cells. Similarly, the percentage of cellular uptake via flow cytometry (Figure 3) confirmed MCF-7 cells incubated with Rhodamine-loaded nanocarrier showed maximum intensity after 2 h (99.72% uptake) and 4 h (100% uptake). No differences were seen in the percentage of cellular uptake with the time elapsed.
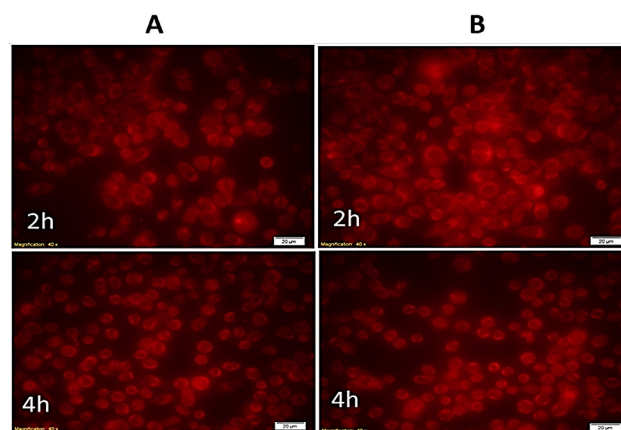
Cytotoxic effects of DOX loaded nanoparticles in MCF-7 cells

MTT assay was used to evaluate the cytotoxic effects of blank NPs, DOX, and DOX loaded NPs in MCF-7 breast cancer cells. Figure 4 showed the effects of all treatments using different concentrations on the proliferation rate of MCF-7 cancer cells. Blank NPs did not exert any significant cytotoxic impact on the proliferation of cancer cells, even at higher concentrations in comparison to DOX and DOX/NPs. This finding approved the safety of cyclodextrin dendritic-graphene oxide NPs for use in *in vivo* investigations. The cytotoxicity of the same concentrations of DOX and DOX loaded NPs were evaluated in MCF-7 cells after a 48 h exposure and results found that the proliferation rate of cells reduced in a time-dependent manner. The *in vitro*

Figure 2: DOX loaded nanocarrier uptake by MCF-7 cells. A. Cells treated with free Rhodamine. B. Cells treated with DOX loaded nanocarrier

treatment with DOX/NPs shifted the cytotoxicity profile to the left, reducing the IC50 and enhancing DOX efficiency when loaded into NPs.

Evaluation of DOX loaded NPs on MCF-7 cell apoptosis

In this study, apoptosis was evaluated in MCF-7s after 48 h via DAPI and MitoTracker Green staining. DAPI staining of MCF-7 cells non-treated and treated with blank NPs showed no significant change in the nuclei of cells, as shown in the fluorescent microscopy images in Figure 5. This confirmed the MTT result on the safety of NPs for *in vivo* studies. DAPI staining indicated the induction of apoptosis in MCF-7 cells after treatment with DOX (P<0.05). MCF-7 cells treated with DOX showed clear apoptotic features with an increase in the number of cells
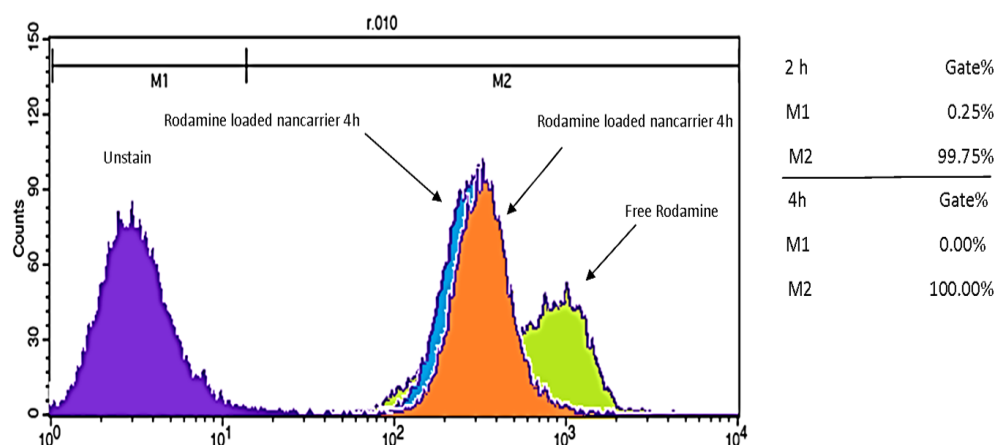
Figure 3: Cellular uptake as a percentage of DOX-nanocarrier by MCF-7 cells, 2 and 4 hours after treatment.
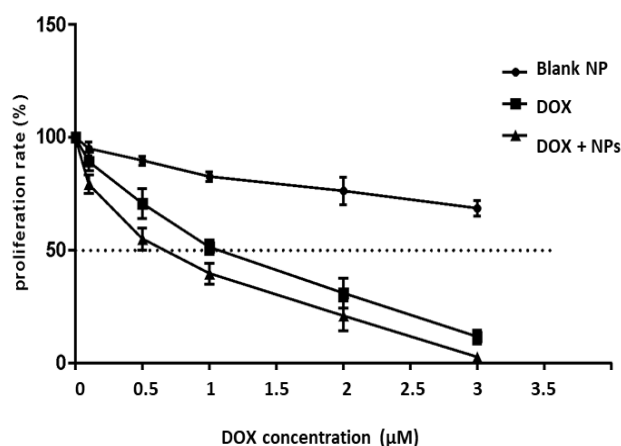

Figure 4: Proliferation rate as a percentage of the control. MCF-7 cells were exposed to varying concentrations of free DOX (DOX), DOX-nanocarrier (DOX + NPs), or free nanocarrier (Blank NP).

with small, condensed nuclei after 48 h, an indication of chromatin fragmentation. More importantly, treatment with DOX loaded NPs resulted in a potent increase in the number of apoptotic cells compared to cells treated with free DOX (P<0.05; Figure 5). In addition to DAPI staining, MitoTracker green staining was also applied to cells treated with various modalities. MitoTracker green is a fluorescent probe used to evaluate mitochondrial mass that binds to the mitochondrial membrane, and thus staining intensity has been considered an index of mitochondrial mass [17]. On the other hand, an increase in mitochondrial mass is a marker of increased apoptosis [18]. Incubation of non-treated control and NPs treated groups with MitoTracker Green staining showed no significant increase in the fluorescence intensity, indicating that the NPs did not induce apoptosis. In addition, cells exposed to DOX resulted in higher florescence intensity, hence increased

mitochondrial mass, and apoptosis in MCF-7 cancer cells (P<0.05). DOX-loaded NPs exerted a more potent impact on inducing apoptosis than DOX alone (P<0.05; Figure 5).

Cytotoxic effects of DOX loaded nanoparticles *in vivo*

Chemotherapeutic-induced toxic side effects on healthy tissues such as heart, kidney and liver are considered one of the most critical challenges in the successful treatment of cancer. DOX has a critical role in the treatment of various human malignancies, including breast cancer. Cardiotoxicity, nephrotoxicity and hepatotoxicity are the most-reported side effects of DOX therapy [19]. The application of nanocarriers and nano-based drug delivery systems is appropriate for carrying chemotherapeutics such as DOX in the systemic circulation to overcome off-target side effects. In our study, MTT assay showed loading DOX into NPs reduced the IC50 value of DOX in MCF-7 breast cancer cells in comparison to free DOX, which indicates the efficacy of designed NPs in decreasing the DOX-mediated toxic impact on healthy cells and tissues, as well as killing cancer cells. For evaluating the possible cytotoxic effects of synthesized NPs on healthy tissues, we injected blank NPs, Free DOX and DOX loaded NPs into healthy rats and the serum levels of biochemical parameters related to heart, kidney and liver damage were measured four days after injection. Liver injury was evaluated by measuring the serum levels of AST and ALT. In the animals which received blank NPs, the serum levels of these two enzymes were comparable to controls, an indicator of the safety of the synthesized NPs on the liver. As shown in figure 6, DOX resulted in the significant elevation of AST and ALT serum levels due to drug-induced liver damage (P<0.05). However, DOX-loaded NPs
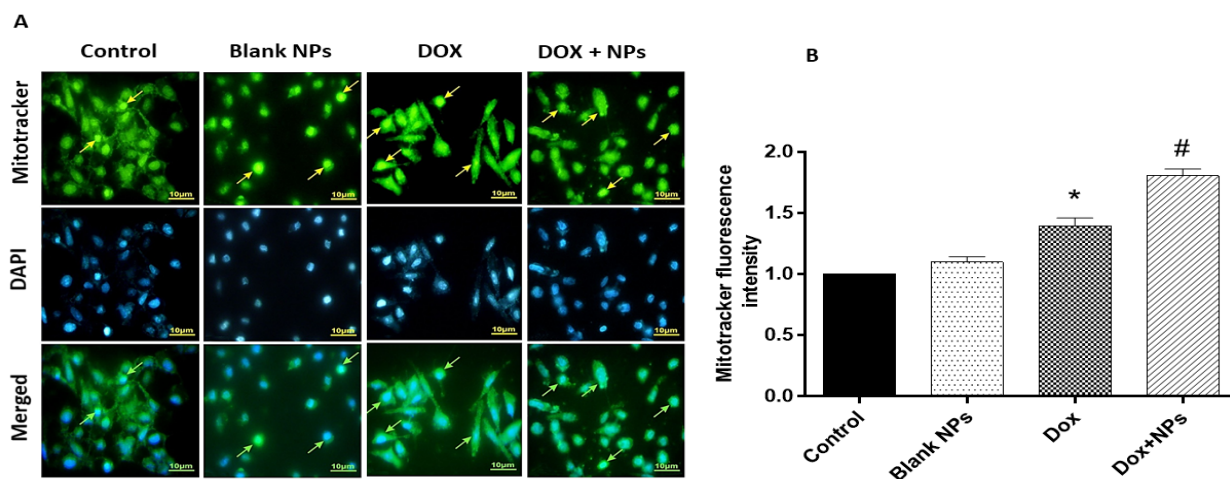
Figure 5: The effects of treatment with free DOX, DOX-nanocarrier (DOX + NPs), and free nanocarrier (Blank NPs) on apoptosis in MCF-7 cells after 48 hours. A. Percentage of apoptotic cells revealed by MitoTracker Green assay, with representative photomicrographs with the nucleus of apoptotic cells labeled in light brown. B. Quantitative analysis of MitoTracker fluorescence intensity in groups. The results are expressed as mean ± SD values from at least 3 independent experiments. * $P < 0.05$ for DOX treated group in comparison to control group, # $P < 0.05$ for DOX+NPs treated group in comparison to DOX group.

alleviated AST and ALT levels, hence, reducing potential liver damage. The effects of different treatments on heart tissue were also investigated by measuring serum levels of LDH and CK, markers of cardiac damage. As similar to liver parameters, blank NPs did not exert significant effect on the serum levels of LDH and CK. DOX resulted in a significant increase in LDH and CK serum levels, when compared to controls ($P<0.05$; Figure 6). In comparison to DOX, the serum levels of LDH and CK were significantly lower with DOX-loaded NPs, indicating that DOX loaded NPs induce less toxicity on cardiac tissue in comparison to free DOX ($P<0.05$). Finally, serum levels of BUN and Cr were also evaluated in our study in order to assess kidney toxicity. No significant change was found in serum levels of these two markers in NPs-treated rats. DOX treatment resulted in a significant increase in BUN and Cr levels as compared to controls. DOX/NPs led to reduced BUN and Cr levels, and therefore less kidney damage ($P<0.05$; Figure 6). Our synthesized nanocarriers were successfully reduced the toxic effects of DOX in the liver, heart, and kidney tissues of rats.

Discussion

Breast cancer is one of the most common malignancies diagnosed in women worldwide. There is a need for the development of novel and more effective treatments which aim to reduce the toxic side effects of systemic chemotherapeutic drugs. In this study, we evaluated the effectiveness of DOX loaded magnetism nanoparticles based on cyclodextrin dendritic-graphene oxide in MCF-7 breast cancer cells. The current study showed that DOX loaded NPs effectively inhibited cellular proliferation, increased DOX efficacy, and induced apoptosis in the MCF-7 cell line. In addition, DOX/NPs reduced DOX mediated cytotoxic effects on heart, liver and kidney in a healthy rat model.

DOX is widely used for the treatment of digestive system cancers and is a potent inhibitor of DNA synthesis in cancer cells but suffers from drug resistance, short half-life and dose dependent toxicity [20]. With the aim of developing a drug delivery system and increasing the effectiveness of common chemotherapeutic agents, nanocarriers constitute a step forward in improving treatments [21]. In this study, we used β-cyclodextrin functionalized dendrimeric graphene oxide-magnetic nanoparticles as a DOX carrier. These nanoparticles have a higher drug loading capacity and low off-site toxicity, which initially reduced cellular proliferation which is considered an important property in effective cancer therapy. Importantly, our fabricated nanoparticles containing DOX were efficiently taken up by MCF-7 cells and it was assumed that the improved internalization, was at least in part, responsible for the increased inhibition of cellular proliferation. Ahmadi et al [22] investigated the cellular uptake, biocompatibility and beneficial effects of methotrexate loaded pH-responsive cationic cyclodextrin coated magnetic nanoparticles in an osteosarcoma cell line and reported that their nano-system has potential
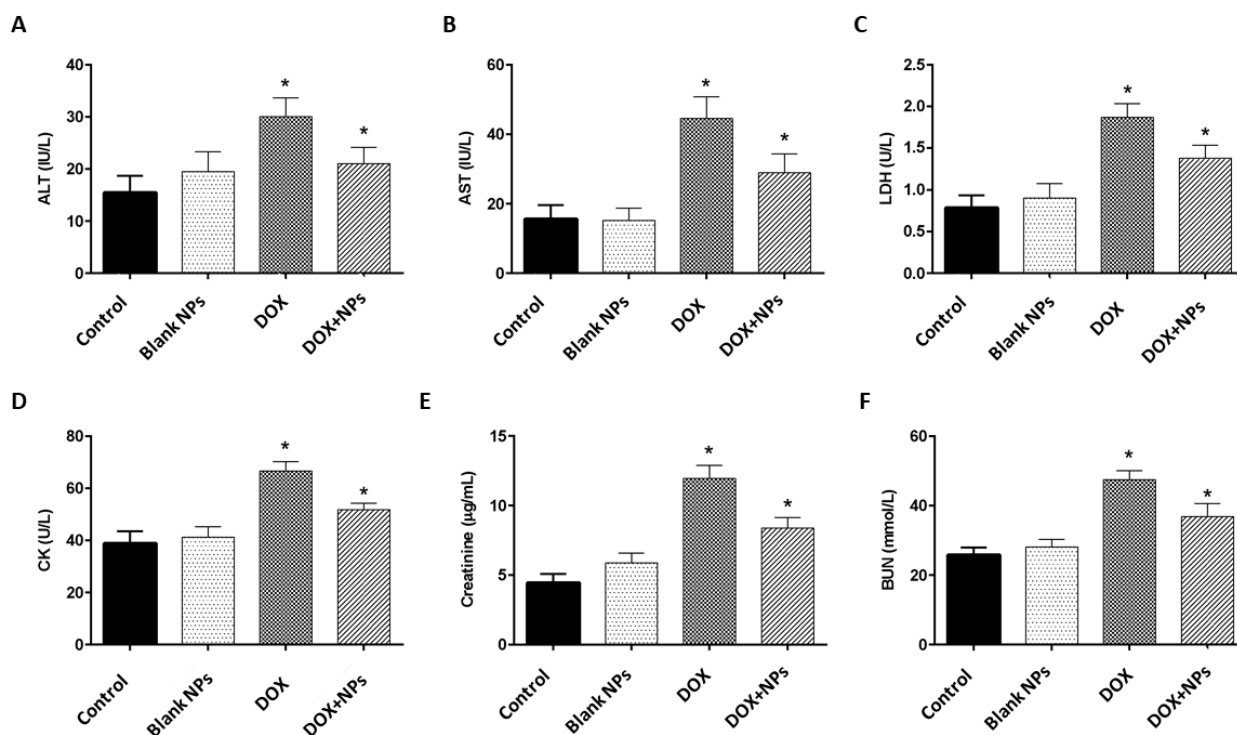
Figure 6: Serum levels of biochemical parameters in rats after treatment with free DOX, DOX-nanocarrier (DOX + NPs), and free nanocarrier (Blank NPs). A. Alanine aminotransferase (ALT), B. Aspartate aminotransferase (AST), C. Lactate dehydrogenase (LDH), D. Creatine kinase (CK), E. Creatinine and F. Blood urea nitrogen (BUN) in experimental groups. The values are represented as mean ± SD (n = 6 animals in each group). * P < 0.05, when compared to controls.

for effective drug delivery but with the need for further evaluation [22].

It has been widely acceptance that drug delivery systems induce effective apoptosis in cancer cells and, consistent with this notion, we further demonstrated that DOX-loaded nanoparticles more potently induce apoptosis in cancer cells. Our results were similar to Khelghati et al [23], which evaluated the effects of DOX loaded pH-sensitive magnetic hyperbranched β-cyclodextrin in an osteosarcoma cell line. Their smart nano-system was biocompatible, with improved release in acidic pH and more potently induced apoptosis compared to free DOX, and may be a suitable delivery system for DOX in the treatment of bone cancer [23]. Interestingly, we found that DOX-loaded nanoparticles produced less cardiotoxicity, nephrotoxicity and hepatotoxicity compared to free DOX in rats, which is considered a major problem with the use of DOX. Our results are consistent with Shafiei et al [24] which showed that DOX/NPs treated mice had no toxic effects on healthy tissues, while, reducing the toxic side effects of DOX by improved cellular internalization [24].

Here we have used a drug delivery system based on graphene oxide nanocarriers for the controlled release

of DOX in MCF-7 cancer cells. Our results showed that DOX/NPs increased the efficacy of DOX by increasing the inhibition of cellular proliferation and inducing apoptosis. The fabrication of DOX/NPs decreased off-target side effects of the drug *in vivo*. We believe our modified graphene oxide NPs could sensitize breast cancer cells to DOX and recommend further *in vivo* testing.

Conflict of interest: Authors state no conflict of interest.

Data Availability Statement: The datasets generated during and analysed during the current study are available from the corresponding author on reasonable request.

References

1. Sambi M, Qorri B, Harless W, Szewczuk MR. Therapeutic options for metastatic breast cancer. Breast Cancer Metastasis and Drug Resistance. Springer; 2019. pp. 131–72.
2. Havas M. Integrative Therapeutic Options for Treating Stage Four Breast Cancer. Clin Oncol. 2019;4:1607.
3. Lovitt CJ, Shelper TB, Avery VM. Doxorubicin resistance in breast cancer cells is mediated by extracellular matrix proteins. BMC Cancer. 2018 Jan;18(1):41.

4. Zhang J, Zhang D, Li Q, Jiang Y, Song A, Li Z, et al. Task-Specific Design of Immune-Augmented Nanoplatform to Enable High-Efficiency Tumor Immunotherapy. ACS Appl Mater Interfaces. 2019 Nov;11(46):42904–16.

5. Zhang H, Jiang W, Liu R, Zhang J, Zhang D, Li Z, et al. Rational design of metal organic framework nanocarrier-based codelivery system of doxorubicin hydrochloride/verapamil hydrochloride for overcoming multidrug resistance with efficient targeted cancer therapy. ACS Appl Mater Interfaces. 2017 Jun;9(23):19687–97.

6. Chen X, Zhang X, Li S, Zhang L, Zhang Q, Chen Z, et al. Engineering of Yin Yang-like nanocarriers for varisized guest delivery and synergistic eradication of patient-derived hepatocellular carcinoma. Nanoscale Horiz. 2019;4(5):1046–55.

7. Tian Y, Guo R, Jiao Y, Sun Y, Shen S, Wang Y, et al. Redox stimuli-responsive hollow mesoporous silica nanocarriers for targeted drug delivery in cancer therapy. Nanoscale Horiz. 2016 Nov;1(6):480–7.

8. Shafei A, El-Bakly W, Sobhy A, Wagdy O, Reda A, Aboelenin O, et al. A review on the efficacy and toxicity of different doxorubicin nanoparticles for targeted therapy in metastatic breast cancer. Biomed Pharmacother. 2017 Nov;95:1209–18.

9. Hossen S, Hossain MK, Basher MK, Mia MN, Rahman MT, Uddin MJ. Smart nanocarrier-based drug delivery systems for cancer therapy and toxicity studies: A review. J Adv Res. 2018 Jun;15:1–18.

10. Zhang H, Liu XL, Zhang YF, Gao F, Li GL, He Y, et al. Magnetic nanoparticles based cancer therapy: current status and applications. Sci China Life Sci. 2018 Apr;61(4):400–14.

11. Wakaskar R. Types of nanocarriers–formulation method and applications. J Bioequiv Availab. 2017;9:10000e77.

12. Zhu L, Zhou Z, Mao H, Yang L. Magnetic nanoparticles for precision oncology: theranostic magnetic iron oxide nanoparticles for image-guided and targeted cancer therapy. Nanomedicine (Lond). 2017 Jan;12(1):73–87.

13. Yang YF, Meng FY, Li XH, Wu NN, Deng YH, Wei LY, et al. Magnetic graphene oxide-Fe3O4-PANI nanoparticle adsorbed platinum drugs as drug delivery systems for cancer therapy. J Nanosci Nanotechnol. 2019 Dec;19(12):7517–25.

14. Pooresmaeil M, Namazi H. β-Cyclodextrin grafted magnetic graphene oxide applicable as cancer drug delivery agent: synthesis and characterization. Mater Chem Phys. 2018;218:62–9.

15. Makharza SA, Cirillo G, Vittorio O, Valli E, Voli F, Farfalla A, et al. Magnetic graphene oxide nanocarrier for targeted delivery of cisplatin: a perspective for glioblastoma treatment. Pharmaceuticals (Basel). 2019 May;12(2):76.

16. Ahmadi D, Zarei M, Rahimi M, Khazaie M, Asemi Z, Mir SM, et al. Preparation and in-vitro evaluation of pH-responsive cationic cyclodextrin coated magnetic nanoparticles for delivery of methotrexate to the Saos-2 bone cancer cells. 2020:101584. https://doi.org/10.1016/j.jddst.2020.101584.

17. Petrovas C, Mueller YM, Dimitriou ID, Altork SR, Banerjee A, Sklar P, et al. Increased mitochondrial mass characterizes the survival defect of HIV-specific CD8+ T cells. 2007;109(6):2505-13.

18. Apostolova N, Gomez-Sucerquia LJ, Moran A, Alvarez A, Blas-Garcia A, Esplugues JJBjop. Enhanced oxidative stress and increased mitochondrial mass during efavirenz-induced apoptosis in human hepatic cells. 2010;160(8):2069-84.

19. Gelen V, Şengül E, Yıldırım S, Atila GJIjobms. The protective effects of naringin against 5-fluorouracil-induced hepatotoxicity and nephrotoxicity in rats. 2018;21(4):404.

20. Sun J, Zhang L, Zhang Y, Yue CW, Lin J, Wang H, et al. Smart albumin-loaded Rose Bengal and doxorubicin nanoparticles for breast cancer therapy. J Microencapsul. 2019 Dec;36(8):728–37.

21. Khalid A, Bashir S, Sohail M, Amirzada MI. Characterization of doxorubicin nanoparticles prepared by ionic gelation. Trop J Pharm Res. 2018;17(12):2329–34.

22. Ahmadi D, Zarei M, Rahimi M, Khazaie M, Asemi Z, Mir SM, et al. Preparation and in-vitro evaluation of pH-responsive cationic cyclodextrin coated magnetic nanoparticles for delivery of methotrexate to the Saos-2 bone cancer cells. J Drug Deliv Sci Technol. 2020;57:101584.

23. Khelghati N, Rasmi Y, Farahmandan N, Sadeghpour A, Mir SM, Karimian A, et al. Hyperbranched polyglycerol β-cyclodextrin as magnetic platform for optimization of doxorubicin cytotoxic effects on Saos-2 bone cancerous cell line. J Drug Deliv Sci Technol. 2020;57:101741.

24. Shafiei-Irannejad V, Rahimi M, Zarei M, Dinparast-Isaleh R, Bahrambeigi S, Alihemmati A, et al. Polyelectrolyte carboxymethyl cellulose for enhanced delivery of doxorubicin in MCF7 breast Cancer cells: toxicological evaluations in mice model. Pharm Res. 2019 Mar;36(5):68.